

Adsorption behaviour of As(III) onto synthetic iron-based minerals: A comparative study of akaganeite, goethite and magnetite

Justyna Ulatowska

Department of Process Engineering and Technology of Polymers and Carbon Materials, Wrocław University of Science and Technology, Wybrzeże Wyspiańskiego Street 27, Wrocław, Lower Silesia 50-370, Poland

Corresponding author: justyna.ulatowska@pwr.edu.pl

Abstract: The present study compares the adsorption capacity of iron-based minerals in removing As(III) from aqueous solutions. The work contains the results of studies carried out on a laboratory scale. The synthetic material was used in three forms as akaganeite, goethite and magnetite. To characterise the minerals before and after adsorption of As(III), specific surface area, particle size distribution, density, and zeta potential were determined. Additionally, digital and optical micrographs, SEM, and FTIR analyses were performed. In the experimental part, the influence of the main parameters on the adsorption efficiency was investigated (pH, initial concentration, contact time, and amount of adsorbent). Adsorption isotherms were fitted by Freundlich, Langmuir, and Dubinin-Radushkevich models. Pseudo-first-order (PFO), pseudo-second-order (PSO), and intraparticle diffusion (IPD) models were used to fit the kinetics data. Linear regression was used to estimate the parameters of isotherm and kinetic models. FTIR measurements gave helpful information on the synthesised minerals and the As(III) removal process. Results show that As(III) adsorption is related to the iron-based adsorbents, and adsorption efficiency increases in the following order: goethite < magnetite < akaganeite.

Keywords: iron-based minerals, arsenic, adsorption, FTIR analysis, kinetic study

1. Introduction

Arsenic is present in almost all Earth's subsystems and, in terms of prevalence, ranks twentieth among the elements found in the earth's crust. It forms part of more than two hundred minerals, the best known of which is arsenopyrite (Bhandari et al., 2012). In the aquatic environment, depending on the pH and the prevailing oxidation-reduction conditions, arsenic can occur in compounds on -3, 0, +3 and +5 oxidation levels. In groundwater, due to the anaerobic conditions, arsenic is most often present in the form of H_3AsO_3 , H_3AsO_3^- , $\text{H}_3\text{AsO}_3^{2-}$, AsO_3^{3-} , while in well-oxygenated surface waters it occurs mainly in the forms H_3AsO_4 , H_2AsO_4^- , HAsO_4^{2-} and AsO_4^{3-} (Mondal & Garg, 2017; Hao et al., 2018).

Contamination of natural water resources with toxic arsenic compounds is often associated with the mining industry, in particular with the exploitation activities of gold or copper mines (Eisler, 2004). A serious threat to the environment, related to the process of extraction of these metals, is the discharge of significant amounts of wastewater containing large quantities of arsenic ions into receiving bodies of water. Acidification of these waters and their considerable salinity caused by the presence of sulphate ions is also a problem (Wolkersdorfer & Bowell, 2005). Therefore, an appropriate level of treatment and continuous monitoring of the composition of mine waters discharged to receivers in the area where mining works are carried out is fundamental to preserve local ecosystems.

The intensification of activities for sustainable development and operativeness of the mining industry observed in recent years is connected with raising environmental protection standards and introducing mining processes at a high technological level that are more environmentally friendly, but at the same time, are cheap and safe. Mining companies are thus forced to look for sufficiently

effective water and wastewater treatment methods to reduce the negative impact on the aquatic environment.

Most popular, precipitation methods are mainly used to remove arsenic compounds from wastewater from the mining industry (Langsch et al., 2012). Much attention is paid to adsorption and ion exchange processes, which are primarily used to purify or treat water containing small amounts of arsenic. Among the available adsorption and ion exchange materials for removing As(III) and As(V), an important group are materials primarily composed of iron compounds. The literature has repeatedly confirmed the suitability of iron oxides and hydroxides for the treatment of water and wastewater containing toxic arsenic compounds (Daus et al., 2004; Kanel et al., 2005; Deliyanni et al., 2009; Kolbe et al., 2011; Ghosh et al., 2012; Szlachta & Wójtowicz, 2016; Hao et al., 2018; Polowczyk et al., 2018; Ajith et al., 2021). Additionally, there are many reports in the literature showing the use of iron-based adsorbents to remove other toxic anions, heavy metal ions or organic compounds (Mustafa et al., 2004; Wang et al., 2010; Mohapatra et al., 2010; Kim et al., 2011; Zhao et al., 2012; Kyzas et al., 2013; Lasheen et al., 2015; Dube et al., 2016; Nguyen et al., 2021; Shi et al., 2021; Szewczuk-Karpisz et al., 2021).

When designing adsorption systems, it is necessary to know the adsorption kinetics, which determines the process's rate. Most commonly, adsorbent-adsorbate interactions are approximated by pseudo-first-order (PFO), pseudo-second-order (PSO), Elovich or intraparticle diffusion models (Ghosh et al., 2012). On the other hand, adsorption equilibrium are described by well-known isotherms such as Freundlich, Langmuir, Freundlich-Langmuir, Radke-Prausnitz, Dubinin-Kaganer-Radushkevich, etc. (Deliyanni et al., 2009). How given literature, Freundlich (Deliyanni et al., 2006) and Langmuir (Kolbe et al., 2011; Mamindy-Pajany et al., 2011; Polowczyk et al., 2018) equations are most commonly used to describe the adsorption equilibrium of As(III) on iron-based minerals.

This study evaluated the efficiency of As(III) adsorption from model aqueous solutions using three synthetic iron compounds: akaganeite, goethite, and magnetite. The adsorbent dose, pH, contact time and initial As(III) concentration has been investigated. Additionally, the materials obtained before and after As(III) adsorption were characterised to determine the probable mechanism of disposal of As(III) ions.

2. Materials and methods

2.1. Synthesis of iron-based minerals

2.1.1. Akaganeite

An 8.11 g of FeCl_3 was dissolved in 500 cm^3 of deionised water (the initial pH of the solution was 1.1). To the solution in a 2 dm^3 beaker, 0.1 M NaOH was slowly added until the pH of the mixture reached about 10. During NaOH addition, the mixture was stirred using a magnetic stirrer. After getting the required pH, the mixture was stirred for 1 hour. The precipitate formed was separated from the solution by centrifugation. The separated residue was then washed with deionised water until neutralised and finally dried in air at room temperature (25°C).

2.1.2. Goethite

A 1 M NaOH was dropped to a mixture of 0.5 M FeSO_4 and 0.1 M $\text{Fe}_2(\text{SO}_4)_3$ in a 1000 cm^3 beaker. During the addition of NaOH, the solution was stirred with a magnetic stirrer. NaOH was added until the pH of the mixture reached about 7-8. After getting the required pH, the mixture was stirred for 1 hour. The precipitate was then separated from the solution by centrifugation. The separated residue was then washed with deionised water until neutralised and finally dried in air at room temperature (25°C).

2.1.3. Magnetite

In 100 cm^3 of deionised water 6.1 g $\text{FeCl}_3 \cdot 6\text{H}_2\text{O}$ and 4.2 g $\text{Fe}_2\text{SO}_4 \cdot 7\text{H}_2\text{O}$ were dissolved and then heated to 90°C. Once the desired temperature was reached, a mechanical stirring of the solution began, and 10 cm^3 of ammonia water (25%) was added. The stirring was continued for another 30 minutes

maintaining the temperature mentioned above conditions. After this time, the mixture was cooled to room temperature. The black magnetite precipitate formed during the reaction was washed several times with water and then maximally separated from it using neodymium magnet discs. The resulting wet deposit of nanoparticles was dried at 40°C.

After drying, all synthetic products were gently crushed and ground with a mortar to obtain a powder to facilitate dosing.

2.2. Characterisation of iron-based minerals

The specific surface area of synthetic iron-based adsorbents (akaganeite, goethite and magnetite) was measured by the Brunauer-Emmett-Teller (BET) method for the helium/nitrogen mixture by using a FlowSorb 2300 apparatus (Micromeritics Instruments Corp, Norcross, GA, USA). The particle size distribution of the investigated materials was determined using an LS13320XR Particle Size Analyzer (Beckman Coulter, Brea, CA, USA). The density of synthetic materials was determined using a pycnometer. The images were taken using an Axio Imager.M1m optical microscope (Zeiss, Jena, Germany) and a JSM-6610LV scanning electron microscope (JEOL Ltd., Akishima, Japan) after sputtering the samples with carbon using an automatic coating machine JEC-530 (JEOL Ltd., Akishima, Japan). The chemical structures of three compounds before and after adsorption of As(III) were monitored by infrared spectroscopy applying Fourier Transformation (FTIR) on a VERTEX 70v spectrometer (Bruker, Billerica, MA, USA). The isoelectric point (pH_{iep}) was determined by electrophoretic zeta potential measurements using a Zetasizer 2000 (Malvern Instruments Ltd., Malvern, UK).

2.3. Adsorbate

Arsenic trioxide (As_2O_3) was used as the source of As(III) ions. A stock solution (1000 mg dm^{-3}) was prepared in deionised water in the presence of NaOH. The so-prepared solution was acidified with 2.0 mol dm^{-3} HCl and diluted to 1 dm^3 with deionised water.

2.4. Analysis

The concentration of As(III) was analysed spectrophotometrically using UV-visible spectrophotometer Evolution 201 (Thermo Fisher Scientific, Madison, USA) by means of the molybdenum blue method, according to standard procedure. The adsorption As(III) capacity of adsorbents was calculated using the equation (1):

$$q = \frac{(c_0 - c) \cdot V}{m} \quad (1)$$

The percentage removal of As(III) was calculated using equation (2):

$$R = \frac{(c_0 - c)}{c_0} \cdot 100\% \quad (2)$$

2.5. Adsorption studies

All the adsorption studies were carried out using the batch method at room temperature for 24 hours. The effect of pH experiment was carried out using 25 mg of an adsorbent (akaganeite, goethite or magnetite) introduced into 10 cm^3 of an aqueous solution of As(III) with a concentration of 100 mg dm^{-3} , the pH of the solutions ranged between 2-12. The pH adjustment of the aqueous As(III) solutions was performed with 0.1 M HCl and 0.1 M NaOH using a pH meter (Elmetron CX-505). The effect of adsorbent dose was studied by varying the amount of an adsorbent (akaganeite, goethite or magnetite) from 5 to 100 mg for initial concentrations of 100 mg dm^{-3} . The effect of contact time was conducted in batch mode by shaking 25 mg of an adsorbent (akaganeite, goethite or magnetite) with As(III) solution (100 mg dm^{-3}). The As(III) concentration was monitored for 24 hours, starting from the second minute of the process. The effect of initial As(III) concentration was carried out using 25 mg of an adsorbent (akaganeite, goethite or magnetite), introduced into 10 cm^3 of As(III) solutions that concentration was varied in the range of 1-100 mg dm^{-3} .

3. Results and discussion

3.1. Characterisation of iron-based minerals

The morphology and particle size of the produced iron-based minerals were observed using a digital camera, optical and scanning electron microscope. The obtained images are shown in Fig. 1. The iron-based minerals obtained by synthesis have standard colouration. Akaganeite is brownish-red, goethite is yellowish-green, and magnetite is black. In addition, it was observed that magnetite is the only one with magnetic properties that help separate the adsorbent from the solution. The particle size of iron-based minerals is evident in optical microscope images. Particles several hundred nanometers in size are visible next to aggregates of about a few tens of microns. Akaganeite has both fine particles and larger particles (Fig. 1B). In contrast, the size and shape of goethite and magnetite are similar (Fig. 1E and Fig. 1H). The particle size was confirmed by the particle size distribution analysis performed for each mineral. The characteristic parameters of the particle size distribution are included in Table 1 along with the basic textural parameters of the obtained iron-based minerals.

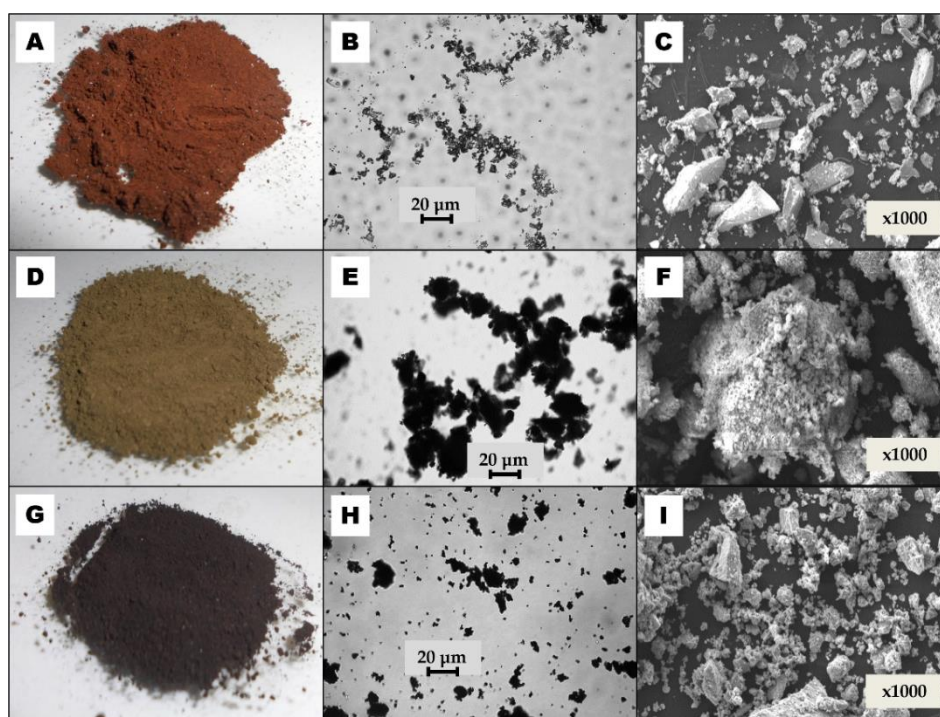


Fig. 1. Images of synthetic iron-based minerals taken with a digital camera (A, D, G), an optical microscope (B, E, H) and a scanning electron microscope (C, F, I); viewed from above: akaganeite (A-C), goethite (D-F) and magnetite (G-I)

Table 1. Chemical and physical properties of synthetic iron-based minerals

Iron-based minerals	SSA* (m ² g ⁻¹)	PSD** (mm)	kurtosis	skewness	span	density (g cm ⁻³)	pH _{iep}
akaganeite	236.5	d ₁₀ 2.27	13.0	3.11	4.95	3.45	8.2
		d ₅₀ 18.8					
		d ₉₀ 95.4					
goethite	13.75	d ₁₀ 5.02	2.91	1.86	36.5	4.37	6.9
		d ₅₀ 20.3					
		d ₉₀ 188.4					
magnetite	36.94	d ₁₀ 5.69	3.29	4.48	4.29	5.35	7.7
		d ₅₀ 50.8					
		d ₉₀ 223.8					

* SSA the specific surface area; **PSD the particle-size distribution

Data in Table 1 indicate that akaganeite has the most developed specific surface area, followed by magnetite, and goethite has the least developed specific surface area. Therefore, it can be emphasised that using akaganeite will obtain higher process efficiencies than when using the other two materials. The determined particle size distributions analysis shows that the produced iron-based adsorbents are characterised by a wide particle size distribution (span > 4). Additionally, kurtosis and skewness were determined. Kurtosis is a measure of the concentration of the obtained results. Its positive values indicate that there is a leptokurtic distribution, i.e. a slender distribution. Skewness, on the other hand, is a measure of the asymmetry of the distribution. Positive values suggest that the distributions are right-skewed.

Zeta potential measurements are essential to determine the surface potential of these adsorbents. The results showed that the negative charge and thus the negative potential increases with increasing pH and reaches a pH 11.5 maximum value of -44.2 , -41.7 and -32.8 mV for akaganeite, goethite, and magnetite, respectively. At acidic pH, the zeta potential of the tested iron-based minerals is positive. At pH 3.5, it takes the highest value of $+32.3$, $+18.2$ and $+15.2$ mV for akaganeite, goethite, and magnetite, respectively. As informed by Schwertmann & Cornell and Hao & co-workers, iron minerals usually have so-called points of zero charge at neutral pH, and therefore they are often used as adsorbents for both anions and cations removal (Schwertmann & Cornell, 2000; Hao et al., 2018). For synthetic iron-based adsorbents, the isoelectric point (pH_{iep}) was found around 8.2, 6.9 and 7.7 for akaganeite, goethite and magnetite, respectively.

3.2. Adsorption analysis

3.2.1. Effect of adsorbent dose

The adsorbent dose effect is an important parameter that determines the amount of removal and capacity of adsorption. The adsorbent dose for obtained iron compounds varied from 0.5 to 10 g dm^{-3} . Fig. 2 shown the impact of adsorbent dose on removing As(III) from aqueous solutions and adsorption capacity for akaganeite (a), goethite (b) and magnetite (c). As expected, As(III) removal increased, and adsorption capacity decreased with the adsorbent dose. For the solution concentration 100 mg dm^{-3} of As(III), the maximum static uptake of As(III) by iron compounds (akaganeite, goethite and magnetite) was achieved for the minimal possible adsorbent-to-solute ratio of 0.5 g dm^{-3} and was 124.2 , 38.9 and $48.4 \text{ mg}_{\text{As(III)}} \text{ g}^{-1}$ of akaganeite, goethite and magnetite, respectively. The maximum As(III) removal was about 96, 50 and 78 % of akaganeite, goethite and magnetite for the maximal adsorbent-to-solute ratio of 10 g dm^{-3} . All the relationships (Fig. 2) confirm that with increasing adsorbent dose, the adsorption capacity decreases and the percentage removal increases. At a lower concentration of the adsorbent, the number of active sites is larger. However, as the adsorbent dose increases, it becomes tightly packed this can limit diffusion, as the adsorbate has limited access to all free active sites, resulting in a general decrease in efficiency and adsorption capacity (Mondal et al., 2008).

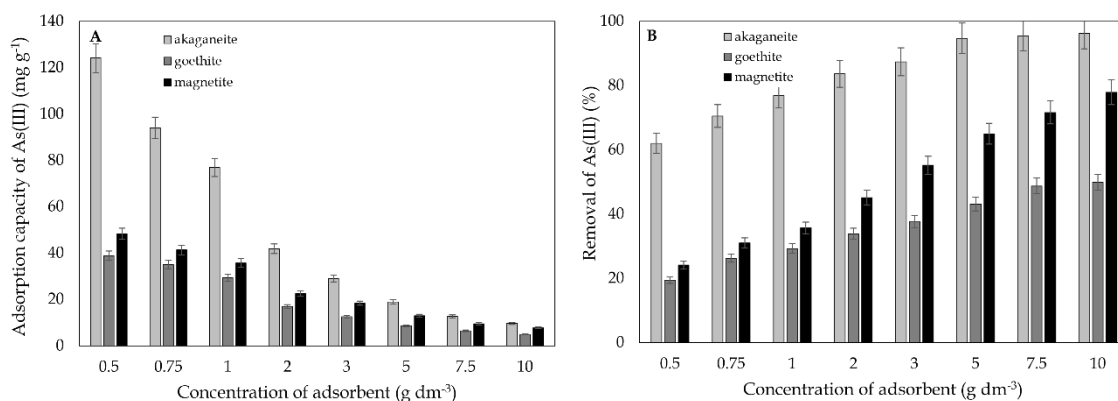


Fig. 2. Effect of adsorbent dose at 100 mg dm^{-3} of initial As(III) concentration on: A - adsorption capacity of As(III) and B - removal of As(III)

3.2.2. Effect of pH

The effect of the pH of the initial solution on the adsorption of As(III) on iron-based minerals was determined in the range from 2 to 12. The results are shown in Fig. 3. The highest As(III) removal from aqueous solutions by iron-based minerals was obtained in acidic conditions (pH about 4). The highest for akaganeite (62%), followed by magnetite (41%) and the lowest removal for goethite (27%). It was also observed that as the pH of the solution increases, the removal of As(III) decreases. At alkaline pH (10-12), the lowest degree of reduction was obtained. For akaganeite it is 19%, for magnetite it is 22%, and for goethite it is less than 5%. A similar trend was observed by Mamindy-Pajany & co-workers, who explored the adsorption of arsenic ions on various commercial iron-based adsorbents (Deliyanni et al., 2009; Mamindy-Pajany et al., 2011). The results showed that higher As(III) removal occurs at moderate pH values, i.e., in the range of 4.0-7.0. However, relatively low As(III) removal is seen at high pH values. As is known, arsenic in aqueous solutions at different pH values can exist in various forms (Hao et al., 2018), and its adsorption strongly depends on the surface charge of the adsorbent. Therefore, the zero charge point (pH_{iep}) of iron-based minerals was also determined to accurately explain the behaviour of As(III) at different pH. The results showed that the obtained adsorbents have pH_{iep} of 8.2, 6.9 and 7.7 for akaganeite, goethite and magnetite, respectively (Table 1). All iron-based materials have positively charged surfaces below the pH_{iep} and negatively charged surfaces above. Therefore, the decrease in percentage removal of As(III) at strongly alkaline pH where the surface is negatively charged can be attributed to electrostatic repulsion because As(III) then exists in negative forms such as $H_2AsO_3^-$ (Lee et al., 2015). In contrast, the decrease at a strongly acidic pH (up to 2.0) can be explained by the fact that arsenic exists as the neutral form - H_3AsO_4 , which makes removing electrostatic attraction to the positively charged surface more difficult (Mudzielwana et al., 2020).

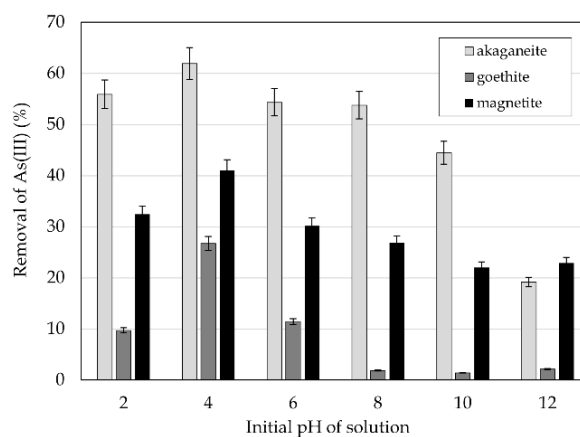


Fig. 3. Adsorption of As(III) onto iron-based adsorbents as a function pH (100 mg dm^{-3} ; 25°C ; dose of adsorbent 25 mg)

3.2.3. Effect of contact time

The effect of contact time on removing As(III) from aqueous solution with the resulting iron compounds was studied at an initial concentration of 100 mg dm^{-3} at room temperature. The dependence of the percentage of removal on time is shown in Fig. 4. It can be seen there that the percentage removal of As(III) from the solution by akaganeite, goethite, and magnetite increased sharply with the contact time until the equilibrium was attained. As shown in Fig. 4, the adsorption took place more rapidly in the initial stages and gradually slowed down as it reached equilibrium. This behaviour is quite common due to the saturation of the available surface active sites. As(III) removal was increased faster during the first 3 hours. After 24 hours, it reached 76, 32 and 42% for akaganeite, goethite and magnetite, respectively. The experiments showed that the equilibrium was reached only after 24 hours for all adsorbents. Therefore, it can be concluded that the active sites on the surface of the adsorbents used were saturated.

The rate-controlling step of adsorption of As(III) ions and investigation of the possible mechanism was determined using three kinetic models. The rate constants were calculated using pseudo-first-order (PFO) and pseudo-second-order (PSO) kinetic models. In contrast, the rate-controlling step was determined using the intraparticle diffusion (IPD) model. The equations of these models are presented in Table 2.

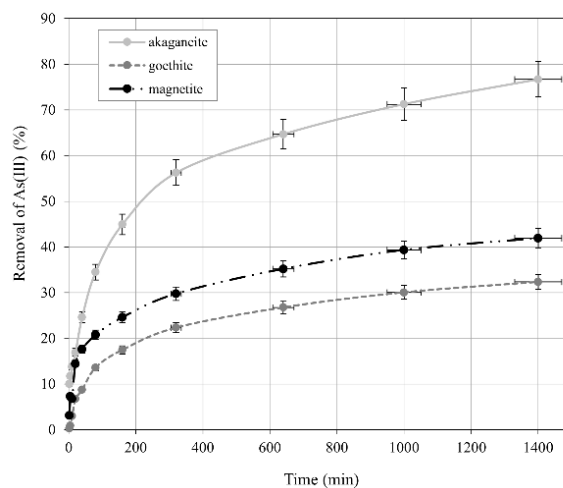


Fig. 4. Adsorption of As(III) onto iron-based adsorbents as a function time (100 mg dm⁻³; 25 °C; dose of adsorbent 25 mg; pH 4.5)

Table 2. List of adsorption kinetics models used in this work

Kinetic model	Equation	Parameters	Reference
PFO	$\log(q_e - q_t) = \log(q_1) - \left(\frac{k_1}{2.303}\right) \cdot t$ (3)	q_1 (mg g ⁻¹) k_1 (min ⁻¹)	(Lagergren, 1898; Ho, 2004; Qiu et al., 2009)
PSO	$\frac{t}{q_t} = \frac{1}{k_2 \cdot q_2^2} + \frac{t}{q_2}$ (4)	q_2 (mg g ⁻¹) k_2 (g mg ⁻¹ min ⁻¹)	(Ho & McKay, 1999; Ho, 2004; Qiu et al., 2009)
IPD	$q_t = k_{IPD} \cdot t^{1/2} + B$ (5)	k_{IPD} (mg g ⁻¹ min ^{-1/2}) B (mg g ⁻¹)	(Weber & Morris, 1963; Qiu et al., 2009; Tsibranska & Hristova, 2011)

Based on the high values of the coefficient of determination (R^2), it can be concluded that the experimental data obtained during the study of the kinetics of As(III) adsorption on iron-based minerals are better described by the pseudo-second-order model than by the pseudo-first-order model. The calculated values of the adsorption capacity from the pseudo-second order model (q_2) are closer to the experimental values (q_{exp}) than from the pseudo-first order model (q_1), thus indicating the chemical nature of the As(III) removal process in the studied systems rather than the physical one. The calculated parameters were presented in Table 3.

Table 3. Kinetic parameters of pseudo-first-order (PFO) and pseudo-second-order (PSO) models

Iron-based minerals	q_{exp} (mg g ⁻¹)	PFO			PSO			
		q_1 (mg g ⁻¹)	k_1 (min ⁻¹)	R^2 (-)	q_2 (mg g ⁻¹)	k_1 (g mg ⁻¹ min ⁻¹)	h (mg g ⁻¹ min ⁻¹)	R^2 (-)
akaganeite	30.69	29.89	$4.28 \cdot 10^{-3}$	0.868	31.15	$4.24 \cdot 10^{-4}$	0.411	0.992
goethite	12.94	13.93	$4.35 \cdot 10^{-3}$	0.871	13.36	$7.44 \cdot 10^{-4}$	0.132	0.991
magnetite	16.78	15.72	$4.27 \cdot 10^{-3}$	0.872	16.93	$8.66 \cdot 10^{-4}$	0.248	0.992

Additionally, the initial adsorption rate defined as $h=k_2 \cdot q_2^2$ was calculated. This parameter was calculated from pseudo-second-order process rate constants and are 0.411, 0.132 and 0.248 $\text{mg g}^{-1} \text{min}^{-1}$ for akaganeite, goethite and magnetite, respectively. They indicate a faster As (III) adsorption process on akaganeite than on the other two adsorbents.

The limiting step of the As(III) adsorption process on iron-based minerals was determined using the Weber-Morris intraparticle diffusion model (Weber & Morris, 1963). The equation of this model was presented in Table 2. The kinetics of intraparticle diffusion was illustrated in Fig. 5 as the relationship of $q_t=f(t^{1/2})$. If adsorption occurred solely by intraparticle diffusion, then the relation $q_t=f(t^{1/2})$ would be rectilinear throughout, and the curve would pass through the origin of the coordinate system. The lack of linearity (broken line on the graph) indicates, in turn, that several processes are involved in the adsorption process and not only intraparticle diffusion. The first steep section corresponds to adsorption on the external surface of the adsorbent grain or the immediate adsorption stage. The second section corresponds to a gradual, gentle adsorption stage, where intraparticle diffusion is the stage that controls the rate of the entire adsorption process (Allen et al., 1989). As shown in Fig. 5, none of the curves are passing through the origin of the coordinate system, suggesting that intraparticle diffusion is not the only limiting step in the process of As(III) adsorption from aqueous solutions on iron-based minerals. In addition, the dependence of q_t on $t^{1/2}$ over the whole time range considered was not rectilinear, clearly indicating that the adsorption rate depends not only on intraparticle diffusion. The calculated k_{IPD} values for individual stages and each adsorbent are summarized in Table 4.

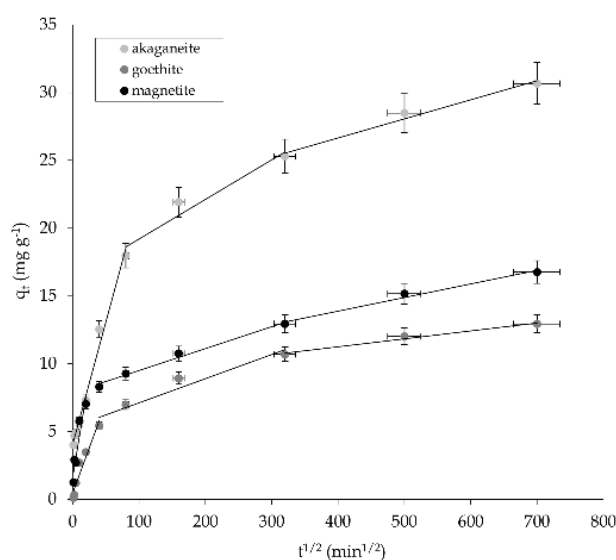


Fig. 5. Intraparticle diffusion model of As(III) adsorption on iron-based minerals (100 mg dm^{-3} ; $25 \text{ }^\circ\text{C}$; dose of adsorbent 25 mg ; $\text{pH } 4.5$)

Table 4. The calculated k_{IPD} values for individual stages of the intraparticle diffusion (IDP)

Iron-based minerals	k_{IPD1} ($\text{mg g}^{-1} \text{min}^{-1/2}$)	k_{IPD2} ($\text{mg g}^{-1} \text{min}^{-1/2}$)	k_{IPD3} ($\text{mg g}^{-1} \text{min}^{-1/2}$)
akaganeite	0.180	0.0292	0.0141
goethite	0.133	0.0179	0.0058
magnetite	0.292	0.0162	0.0101

The calculated k_{IPD} values for individual stages and each adsorbent are summarized in Table 4. The analysis of the obtained results suggests that the limiting stage for the As(III) adsorption process on akaganeite, goethite and magnetite is the third stage. The k_{IPD} values for each of the adsorbents used are lowest in the third stage and indicate that this stage affects the whole process.

3.2.4. Effect of initial concentration

The initial concentration of the various ions is an essential driving force to overcome any resistance to mass transfer between the aqueous and bulk phases. At lower concentrations, all ions in the solution can interact with the adsorbent's binding sites; therefore, the adsorption capacity increases rapidly with increasing initial concentration. At higher concentrations, the adsorption capacity is almost constant due to the saturation of the adsorption site. The Freundlich, Langmuir and Dubinin-Radushkevich isotherm models were used to describe the equilibrium data in this study (Deliyanni et al., 2009; Wang & Guo, 2020). The equations of these models are presented in Table 5. Adsorption isotherms are given in Fig. 6. The calculated parameters of adsorption isotherms along with the coefficient of determination (R^2) are summarized in Table 6.

From obtained isotherms (Fig. 6) and the values of the coefficient of determination (R^2) for selected isotherm models, it can be concluded that the accuracy of the adsorption isotherm models for As(III) removal on iron-based minerals is as follows: Dubinin-Radushkevich > Freundlich > Langmuir.

Using the traditional approach of determining the isotherm parameters by linear regression and evaluating the best-fit form of the isotherm using the R^2 value (Table 6), the Dubinin-Radushkevich isotherm was found to provide the best description and analysis of the experimental data among the models used. Since the best fit to the experimental data was obtained using the DR isotherm equation,

Table 5. List of adsorption isotherm models used in this work

Isotherm model	Equation	Parameters	Reference
Freundlich	$q_e = k_F \cdot c_e^{1/n}$ (6)	$k_F ((\text{dm}^3)^{1/n} \text{mg}^{(1-1/n)} \text{g}^{-1})$ $1/n (-)$	(Freundlich, 1906; Wang & Guo, 2020)
Langmuir	$q_e = \frac{q_L \cdot k_L \cdot c_e}{1 + k_L \cdot c_e}$ (7)	$k_L (\text{dm}^3 \text{mg}^{-1})$ $q_L (\text{mg g}^{-1})$	(Langmuir, 1916; Wang & Guo, 2020)
Dubinin-Radushkevich	$q_e = q_{DR} \cdot \exp(-k_{DR} \cdot \varepsilon^2)$ (8) $\varepsilon = RT \ln \left(\frac{C_0}{c_e} \right)$ (9)	$k_{DR} (\text{mol}^2 \text{kJ}^{-2})$ $q_{DR} (\text{mg g}^{-1})$ $\varepsilon (\text{kJ mol}^{-1})$	(Bering et al., 1972; Foo & Hammed, 2010; Benzaoui et al., 2017)

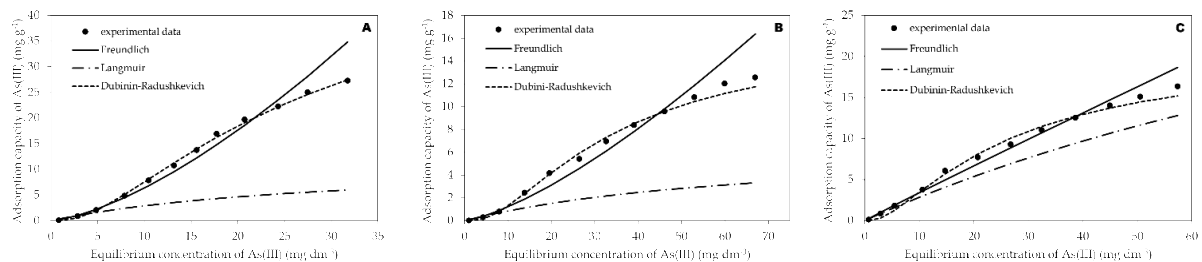


Fig. 6. Adsorption isotherms of As(III) onto akaganeite (A), goethite (B) and magnetite (C) (5-100 mg dm⁻³; 25°C; dose of adsorbent 25 mg; pH 4.5)

Table 6. Parameters of isotherm adsorption models

	Freundlich			Langmuir			Dubinin-Radushkevich		
	k_F $((\text{dm}^3)^{1/n} \text{mg}^{(1-1/n)} \text{g}^{-1})$	$1/n$ (-)	R^2 (-)	k_L $(\text{dm}^3 \text{mg}^{-1})$	q_L (mg g^{-1})	R^2 (-)	k_{DR} $(\text{mol}^2 \text{kJ}^{-2})$	q_{DR} (mg g^{-1})	R^2 (-)
akaganeite	30.7	1.47	0.9851	0.030	13.2	0.9560	$6.18 \cdot 10^{-5}$	45.3	0.993
goethite	12.9	1.38	0.9742	0.015	6.69	0.9301	$7.91 \cdot 10^{-5}$	14.4	0.996
magnetite	16.8	0.985	0.9895	0.006	49.1	0.9856	$4.69 \cdot 10^{-5}$	16.5	0.990

the free energy was determined based on the k_{DR} parameter and the equation (10) (Foo & Hammed, 2010):

$$E = \frac{1}{\sqrt{2 \cdot k_{DR}}} \quad (10)$$

The free energy (E) gives information whether the adsorption type is physical adsorption, ion-exchange or chemical adsorption. If the magnitude of E is lower than 8 kJ mol⁻¹ the adsorption process is of a physical nature, where E is between 8 and 16 kJ mol⁻¹, the adsorption process follows by ion-exchange, and for the greater than 16 kJ mol⁻¹ is chemical adsorption (Benzaoui et al., 2017). The obtained results suggest that the adsorption of As(III) on each of the adsorbents is chemical in nature ($E > 16$ kJ mol⁻¹). The free energy for akaganeite, goethite, and magnetite amount to 89.9, 79.5 and 103.2 kJ mol⁻¹.

3.3. Possible As(III) adsorption mechanism onto iron-based minerals

According to the literature, characteristic bands for individual iron-based minerals can be observed by analysing the FTIR spectra. In Table 7 typical bands for akaganeite, goethite and magnetite are presented (Fu & Quan, 2006; Chirita et al., 2012; Al-Jabri et al., 2018; Çiftçia et al., 2017; Veneranda et al., 2018; Deliyanni et al., 2006; Schwertmann & Cornell, 2000; Zhang & Jia, 2014).

The FTIR spectra of the prepared iron-based minerals before and after As(III) adsorption was shown in Fig. 7. Analysis of FTIR spectra allows identification of the probable mechanism of As(III) adsorption onto iron-based minerals. No change in the structure of synthetic minerals is observable when analysing FTIR spectra before and after adsorption of As(III).

Table 7. Assignment of FTIR absorption bands of the iron-based minerals

Iron-based minerals	Adsorption bands	Interpretation
akaganeite	648 and 693 cm ⁻¹	vibration of hydrogen bonds
	844 cm ⁻¹	chlorine ions in akaganeite
	1620 cm ⁻¹	band from water molecules
	3385-3470 cm ⁻¹	-OH band vibrations
goethite	615-905 cm ⁻¹	stretching vibration FeO
	798 cm ⁻¹	characteristic vibration of goethite
	1650 cm ⁻¹	band from water molecules
	3136-3431 cm ⁻¹	-OH band vibrations
magnetite	588 cm ⁻¹	FeO bands (characteristic bands of magnetite)
	1630 cm ⁻¹	band from water molecules
	3430 cm ⁻¹	-OH band vibration

All samples (akaganeite, goethite and magnetite) before As(III) adsorption had absorption bands in the range 3200-3400 cm⁻¹ and 1630 cm⁻¹ corresponding to -OH and H₂O vibrations, respectively. Most of the bands allowing the identification of iron groups on the FTIR spectrum are in the range of 1000-450 cm⁻¹. In the FTIR spectra of all minerals after As(III) adsorption, an increase in the intensity of the peaks both at 3300 cm⁻¹, 1630 cm⁻¹, and in the range of 450-1200 cm⁻¹ can be observed. In addition, it can be concluded that akaganeite is the most stable mineral because no significant changes in the FTIR spectrum were observed. The characteristic bands are stronger but have not shifted. On the other hand, subtle band shifts can be observed in the spectra of goethite and magnetite.

In order to understand the removal of As(III) ions by iron-based minerals, it is necessary to determine the adsorption mechanism. According to current knowledge, in addition to process parameters such as pH, temperature, initial concentration of As(III) in solution, the adsorbent plays an important role in the adsorption mechanism. As reported by Shi and co-workers, the adsorption mechanism on hydrated iron oxide can be of both cationic and anionic exchange based (Shi et al., 2021).

Analysis of the obtained results and literature reports indicate that iron-based minerals are effective As(III) adsorbents. As reported by Ajith & co-workers and Bhandari & co-workers, the adsorption mechanism of As(III) on goethite is similar to that of As(III) on hematite. The researchers showed that there is then a redox reaction between As(III) (oxidation) and Fe(III) (reduction) (Bhandari et al., 2012; Ajith et al., 2021). For the mechanism of As(III) adsorption on magnetite, Liu & co-workers indicated that As(III) on the magnetite surface forms tridentate hexanuclear corner-sharing complexes (Liu et al., 2015). Whereas Otte & co-workers reported that stable monodentate or bidentate binuclear complexes are formed during adsorption of As(III) on akageneite (Otte et al., 2013).

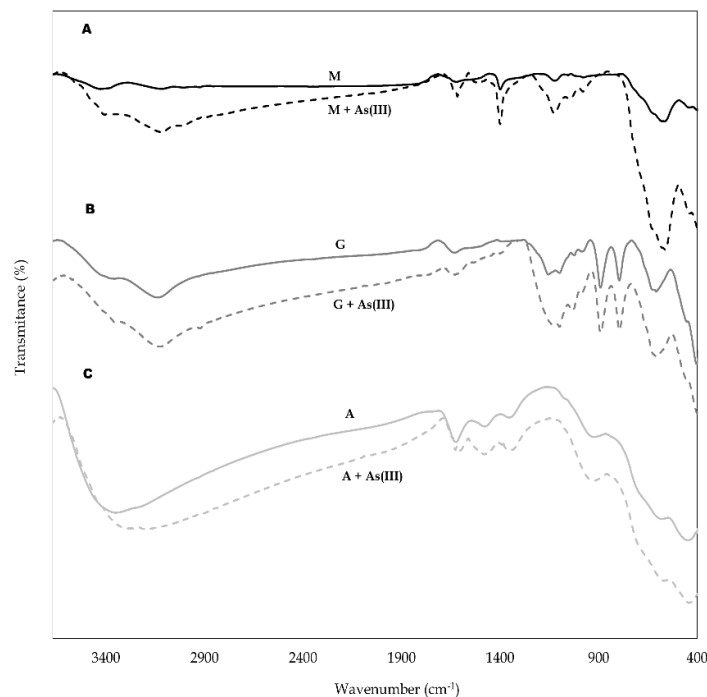


Fig. 7. FTIR spectra of synthetic iron-based minerals before and after As(III) adsorption: A - magnetite; B - goethite; C - akageneite

4. Conclusions

Within the present studies, the As(III) adsorption on synthetic iron-based minerals (akageneite, goethite and magnetite) was assessed. For this purpose, adsorption experiments were performed under different physicochemical conditions (pH, adsorbent dose, initial As(III) concentration and contact time). Results showed that As(III) adsorption rate is related to pH values and initial As(III) concentrations. As(III) adsorption is favoured under acidic pH values and rapidly decreases in basic medium. Adsorption efficiency increases in the following order: goethite < magnetite < akageneite. The As(III) removal efficiency difference of studied materials can be explained by the dissimilarity in specific surface area which is the greatest for akageneite and the lowest for goethite. Another parameter that could be worth investigating to explain these differences is how iron content of these materials influences the efficiency of As(III) removal. The PSO model describes the adsorption kinetics of As(III) onto iron-based minerals better than the PFO model. The IPD model suggested that intraparticle diffusion is not the only rate-limiting step in As(III) adsorption on iron-based minerals. The study of the isotherms adsorption on iron-based minerals is best described by the Dubinin-Radushkevich isotherm model ($R^2 > 0.99$). The obtained free energy suggests that the adsorption of As(III) on each of the adsorbents is chemical in nature.

Nomenclature

t	time (min)
q_e	the amount of Cr(VI) adsorbed at equilibrium (mg g^{-1})

q_t	the amount of Cr(VI) adsorbed at time t (mg g^{-1})
c_e	the equilibrium concentration of Cr(VI) (mg dm^{-3})
c_0	the initial concentration of Cr(VI) (mg dm^{-3})
m	the adsorbent mass (g)
V	the solution volume (dm^3)
q_1	the adsorption capacity of Cr(VI) at equilibrium for pseudo-first-order model (mg g^{-1})
k_1	the rate constant of pseudo-first-order model (min^{-1})
q_2	the adsorption capacity of Cr(VI) at equilibrium for pseudo-second-order model (mg g^{-1})
k_2	the rate constant of pseudo-second-order model ($\text{g mg}^{-1} \text{min}^{-1}$)
k_{IPD}	the intraparticle diffusion rate constant ($\text{mg g}^{-1} \text{min}^{-1/2}$)
B	the parameter related to the thickness of the boundary layer (mg g^{-1})
k_F	the Freundlich constant indicative of the relative adsorption capacity of the adsorbent ($(\text{dm}^3)^{1/n} \text{mg}^{(1-1/n)} \text{g}^{-1}$)
n	the Freundlich equation exponent (-)
q_L	the maximum adsorption capacity in Langmuir model (mg g^{-1})
k_L	the Langmuir constant related to the energy of adsorption ($\text{dm}^3 \text{mg}^{-1}$)
R	the universal gas constant ($\text{kJ mol}^{-1} \text{K}^{-1}$)
T	temperature (K)
q_{DR}	the adsorption capacity in Dubinin-Radushkevich model (mg g^{-1})
k_{DR}	the Dubinin-Radushkevich isotherm constant ($\text{mol}^2 \text{kJ}^{-2}$)
ε	the adsorption potential based on the Polanyi's potential theory (kJ mol^{-1})
E	the free energy (kJ mol^{-1})

Acknowledgments

This research was funded by a subsidy from the Polish Ministry of Science and Higher Education for K25W03D05 of Wroclaw University of Science and Technology, subsidy number 8211104160 (MPK 9030250000).

References

- AJITH, N., SATPATI, A.K., DEBNATH, A.K., SWAIN, K.K., 2021. *Evidences on As(III) and As(V) interaction with iron(III) oxides: Hematite and goethite*. J. Environ. Sci. Health 56, 1007-1018.
- AL-JABRI, M.T.K., DEVI, M.G., AL ABRI, M., 2018. *Synthesis, characterization and application of magnetic nanoparticles in the removal of copper from aqueous solution*. Appl Water Sci 8, 223-230.
- ALLEN, S.J., MCKAY, G., KHADER, K.Y., 1989. *Intraparticle diffusion of basic dye during adsorption onto sphagnum peat*. Environ. Pollut. 50, 39-50.
- BENZAOU, T., SELATNIA, A., DJABALI, D., 2017. *Adsorption of copper (II) ions from aqueous solution using bottom ash of expired drugs incineration*. Adsorp Sci Technol 0, 1-16.
- BERING, B.P., DUBININ, M.N., SERPINSKY, V.V., 1972. *On thermodynamics of adsorption in micropores*. J. Colloid Interface Sci 38, 185-194.
- BHANDARI, N., REEDER, R.J., STRONGIN, D.R., 2012. *Photoinduced oxidation of arsenite to arsenate in the presence of goethite*. Environ. Sci. Technol. 46, 8044-8051.
- CHIRITA, M., BANICA, R., IETA, A., GROZESCU, I., 2012. *Superparamagnetic unusual behavior of micrometric magnetite monodisperse monocrystals synthesized by Fe-EDTA thermal decomposition*. Part. Sci. Technol. 30, 354-363.
- ÇİFTÇİA, H., ERSOYA, B., EVCİN, A., 2017. *Synthesis, characterization and Cr(VI) adsorption properties of modified magnetite nanoparticles*. Acta Phys. Pol. 132, 564-569.
- DAUS, B., WENNRICH, R., WEISS, H., 2004. *Sorption materials for arsenic removal from water, a comparative study*. Water Res. 38, 2948-2954.
- DELIYANNI, E.A., NALBANDIAN, L., MATIS, K.A., 2006. *Adsorptive removal of arsenites by a nanocrystalline hybrid surfactant-akageneite sorbent*. J. Colloid Interface Sci. 302, 458-466.
- DELIYANNI, E.A., PELEKA, E.N., MATIS, K.A., 2009. *Modeling the sorption of metal ions from aqueous solution by iron-based adsorbents*. J. Hazard. Mater. 172, 550-558.

- DUBE, D., PARELCH, C.T., NYONI, B., 2016. *Removal of chromium and nickel from electroplating wastewater using magnetite particulate adsorbent, (1) Effect of pH, contact time and dosage, (2) Adsorption isotherms and kinetics*. MAS 10, 222-232.
- EISLER, R., 2004. *Arsenic hazards to humans, plants, and animals from gold mining*. Rev Environ Contam Toxicol. 180, 133-165.
- FOO, K.Y., HAMMED, B.H., 2010. *Insights into the modeling of adsorption isotherm systems*. Chem. Eng. J. 156, 2-10.
- FREUNDLICH, H.M.F., 1906. *Über die Adsorption Lösungen*. Z. Phys. Chem. 57, 385-470.
- FU, H., QUAN, X., 2006. *Complexes of fulvic acid on the surface of hematite, goethite, and akageneite, FTIR observation*. Chemosphere 63, 403-410.
- GHOSH, M.K., EDDY, G., POINERN, J., ISSA, T.B., SING, P., 2012. *Arsenic adsorption on goethite nanoparticles produced through hydrazine sulfate assisted synthesis method*. Korean J. Chem. Eng. 29, 95-102.
- HAO, L., LIU, M., WANG, N., LI, G., 2018. *A critical review on arsenic removal from water using iron-based adsorbents*. RSC Adv. 8, 39545-39560.
- HO, Y.S., 2004. *Citation review of Lagergren kinetic rate equation on adsorption reactions*. Scientometrics 59, 171-177.
- HO, Y.S., MCKAY, G., 1999. *Pseudo-second order model for sorption processes*. Process Biochem. 34, 451-465.
- KANEL, S.R., MANNING, B., CHARLET, L., CHOI, H., 2005. *Removal of arsenic(III) from groundwater by nanoscale zero-valent iron*. Environ. Sci. Technol. 39, 1291-1298.
- KIM, J., LI, W., PHILIPS, B.L., GREY, C.P., 2011. *Phosphate adsorption on the iron oxyhydroxides goethite (α -FeOOH), akageneite (β -FeOOH) and lepidocrocite (γ -FeOOH), a ^{31}P NMR study*. Energy Environ. Sci. 4, 4298-4305.
- KOLBE, F., WEISS, H., MORGENSTERN, P., WENNRICH, R., LORENZ, W., SCHURK, K., STANJEK, H., DAUS, B., 2011. *Sorption of aqueous antimony and arsenic species onto akageneite*. J. Colloid Interface Sci 357, 460-465.
- KYZAS, G.Z., PELEKA, E.N., DELIYANNI, E.A., 2013. *Nanocrystalline akageneite as adsorbent for surfactant removal from aqueous solutions*. Materials 6, 184-197.
- LAGERGREN, S., 1898. *Zur theorie der Sogenannten adsorption geloster stoffe*. Kungliga Svenska Vetenskapsakademiens. Handlingar 24, 1-24.
- LANGMUIR, I., 1916. *The constitution and fundamental properties of solids and liquids*. J. Am. Chem. Soc. 38, 2221-2295.
- LANGSCH, J.E., COSTA, M., MOORE, L., MORAIS, P., BELLEZZA, A., FALCÃO, S., 2012. *New technology for arsenic removal from mining effluents*. JMR&T 1, 178-181.
- LASHEEN, M.R., EL-SHERIF, I.Y., SABRY, D.Y., EL-WAKEEL, S.T., EL-SHAHAT, M.F., 2015. *Adsorption of heavy metals from aqueous solution by magnetite nanoparticles and magnetite-kaolinite nanocomposite, equilibrium isotherm and kinetic study*. Desalin. Water Treat. 57, 17421-17429.
- LEE, S.M., LALHMUNSIAMA, C., THANHMINGLIANA, TIWANI, D., 2015. *Porous hybrid materials in the remediation of water contaminated with As(III) and As(V)*. Chem. Eng. J. 270, 496-507.
- LIU, C.H., CHUANG, Y.H., CHEN, T.Y., TIAN, Y., LI, H., WANG, M.K., ZHANG, W., 2015. *Mechanism of arsenic adsorption on magnetite nanoparticles from water, Thermodynamic and spectroscopic studies*. Environ. Sci. Technol. 49, 7726-7734.
- MAMINDY-PAJANY, Y., HUREL, C., MARMIER, N., ROMEO, M., 2011. *Arsenic (V) adsorption from aqueous solution onto goethite, hematite, magnetite and zero-valent iron, Effects of pH, concentration and reversibility*. Desalination 281, 93-99.
- MOHAPATRA, M., MOHAPATRA, L., SINGH, P., ANAND, S., MISHRA, B.K., 2010. *A comparative study on Pb(II), Cd(II), Cu(II), Co(II) adsorption from single and binary aqueous solutions on additive assisted nano-structured goethite*. Int. J. Eng. Sci. Technol. 2, 89-103.
- MONDAL, M.K., GARG, R., 2017. *A comprehensive review on removal of arsenic using activated carbon prepared from easily available waste materials*. Environ Sci Pollut Res 24, 13295-13306.
- MONDAL, P., MAJUMDER, C.B., MOHANTY, B., 2008. *Effects of adsorbent dose, its particle size and initial arsenic concentration on the removal of arsenic, iron and manganese from simulated ground water by Fe³⁺ impregnated activated carbon*. J. Hazard. Mater. 150, 695-702.
- MUDZIELWANA, R., GITARI, M.W., NDUNGU, P., 2020. *Enhanced As(III) and As(V) adsorption from aqueous solution by a day based hybrid sorbent*. Green Sustain. Chem. 7, 913.
- MUSTAFA, G., SINGH, B., KOOKANA, R.S., 2004. *Cadmium adsorption and desorption behaviour on goethite at low equilibrium concentrations effects of pH and index cations*. Chemosphere 57, 1325-1333.

- NGUYEN, V.D., NGUYEN, H.T.H., VRANOVA, V., NGUYEN, L.T.N., BUI, Q.M., KHIEU, T.T., 2021. *Artificial neural network modeling for Congo red adsorption on microwave-synthesized akageneite nanoparticles, optimization, kinetics, mechanism, and thermodynamics*. Environ. Sci. Pollut. Res. Int. 28, 9133-9145.
- OTTE, K., SCHMAHL, W.W., PENTCHEVA, R., 2013. *DFT+U Study of arsenate adsorption on β -FeOOH surfaces, Evidence for competing binding mechanisms*. J. Phys. Chem. 117, 15571-15582.
- POLOWCZYK, I., CYGANOWSKI, P., ULATOWSKA, J., SAWIŃSKI, W., BASTRZYK, A., 2018. *Synthetic iron oxides for adsorptive removal of arsenic*. Water Air Soil Pollut 229, 203-213.
- QIU, H., LV, L., PAN, B., ZHANG, Q., ZHANG, W., ZHANG, Q., 2009. *Critical review in adsorption kinetic models*. JZUS A 10, 716-724.
- SCHWERTMANN, U., CORNELL, R.M., 2000. *Iron Oxides in the Laboratory, Preparation and Characterization*. WILEY-VCH Verlag GmbH, Weinheim, Germany, doi,10.1002/9783527613229
- SHI, M., MIN, X., KE, Y., LIN, Z., YANG, Z., WANG, S., PENG, N., YAN, X., LUO, S., WU, J., WEI, Y., 2021. *Recent progress in understanding the mechanism of heavy metals retention by iron(oxyhydr)oxides*. Sci. Total Environ. 752, 141930.
- SZEWCZUK-KARPISZ, K., TOMCZYK, A., CELIŃSKA, M., SOKOŁOWSKA, Z., KUŚMIERZ, M., 2021. *Carboxin and diuron adsorption mechanism on sunflower husks biochar and goethite in the single/mixed pesticide solutions*. Materials 14, 2584.
- SZLACHTA, M., WÓJTOWICZ, P., 2016. *Treatment of arsenic-rich waters using granular iron hydroxides*. Desalin. Water Treat. 57, 26376-26381.
- TSIBRANSKA, I., HRISTOVA, E., 2011. *Comparison of different kinetic models for adsorption of heavy metals onto activated carbon from apricot stones*. Bulgarian Chemical Communications 43, 370 - 377.
- VENERANDA, M., ARAMENDIA, J., BELLOT-GURLET, L., COLOMBAN, P., CASTRO, K., MADARIAGA, J.M., 2018. *FTIR spectroscopic semi-quantification of iron phases, A new method to evaluate the protection ability index (PAI) of archaeological artefacts corrosion systems*. Corrosion Science 133, 68-77.
- WANG, J., GUO, X., 2020. *Adsorption isotherm models, Classification, physical meaning, application and solving method*. Chemosphere 258, 127279.
- WANG, X.S., LU, H.J., ZHU, L., LIU, F., REN, J.J., 2010. *Adsorption of lead(II) ions onto magnetite nanoparticles*. Adsorpt. Sci. Technol. 28, 407-417.
- WEBER, JR., W.J., MORRIS, J.C., 1963. *Kinetics of adsorption on carbon from solution*. J. Sanit. Eng. Div. - ASCE 89, 31-59.
- WOLKERSDORFER, C., BOWELL, R., 2005. *Contemporary reviews of mine water studeie in Europe. Part 2. Mine Water Environ* 24, 2-37.
- ZHANG, Y.X., JIA, Y., 2014. *A facile solution approach for the synthesis of akaganéite (β -FeOOH) nanorods and their ion-exchange mechanism toward As(V) ions*. Appl. Surf. Sci. 290, 102-106.
- ZHAO, J., LIN, W., CHANG, Q., LI, W., LAI, Y., 2012. *Adsorptive characteristics of akageneite and its environmental applications, a review*. Environ. Technol. Rev. 1, 114-126.